

LARGE-EDDY SIMULATION OF AEROSOL TRANSPORT OVER DIFFERENT URBAN LOCAL CLIMATE ZONES

Alexander I. Varentsov^{1,2,3,4*}, Evgeny V. Mortikov^{1,4,5}, Andrey V. Glazunov^{5,1}, Andrey V. Debolskiy^{1,3,4}, Mariya A. Kuzmicheva⁶, Victor M. Stepanenko^{1,2}

¹Research Computing Center, Lomonosov Moscow State University, Leninskie Gory 1, b. 4, 119234, Moscow, Russia

²Faculty of Geography, Lomonosov Moscow State University, Leninskie Gory 1, 119991, Moscow, Russia

³Obukhov Institute of Atmospheric Physics, Russian Academy of Sciences, Pyzhevskiy Pereulok 3, 119017, Moscow, Russia

⁴Moscow Center for Fundamental and Applied Mathematics, Leninskie Gory 1, 119991, Moscow, Russia

⁵Marchuk Institute of Numerical Mathematics, Russian Academy of Sciences, Gubkina 8, 119333, Moscow, Russia

⁶Faculty of Mechanics and Mathematics, Lomonosov Moscow State University, Leninskie Gory 1, 119991, Moscow, Russia

*Corresponding author: aivarentsov98@gmail.com

Received: March 7th 2025 / Accepted: June 5th 2025 / Published: October 1st 2025

<https://doi.org/10.24057/2071-9388-2025-3925>

ABSTRACT. As urban areas grow, understanding the impact of built environments on aerosol distribution is crucial for accurate monitoring and forecasting of urban air quality and for the development of mitigation strategies. This study uses Large Eddy Simulation approach combined with Local Climate Zones (LCZ) classification to simulate the transport of Lagrangian aerosol particles in different urban configurations. The study simulates several urban configurations based on LCZ classification, specifically LCZ 4 (open high-rise), LCZ 5 (open mid-rise), and LCZ 6 (open low-rise), varying in building height and density. Both regular and randomized urban development configurations were examined to understand the impact of building geometry on particle dispersion. The study reveals that building orientation significantly influences particle distribution, with structures parallel to the wind adding horizontal dispersion and those perpendicular promoting vertical mixing. In randomized configurations, variations in particle concentrations highlight the role of architectural heterogeneity in turbulence development and aerosol dispersion. The findings suggest that aggregated block- or district-scale building geometry properties strongly influence aerosol transport. For randomized urban configurations, without idealized regular structures, the difference in the large-scale morphometric characteristics of specified LCZ types has a significantly greater impact on the particle dispersion process than the local geometric differences between configurations of the same LCZ type. Future research taking into account diverse meteorological conditions and more LCZ types is recommended to enhance the accuracy and applicability of this approach.

KEYWORDS: urban air quality, large eddy simulation, local climate zones, aerosol dispersion, Lagrangian particle transport, urban morphology

CITATION: Varentsov A. I., Mortikov E. V., Glazunov A.V., Debolskiy A. V., Kuzmicheva M. A., Stepanenko V. M. (2025). Large-Eddy Simulation Of Aerosol Transport Over Different Urban Local Climate Zones. *Geography, Environment, Sustainability*, 3 (18), 68-79

<https://doi.org/10.24057/2071-9388-2025-3925>

ACKNOWLEDGEMENTS: LES model and LCZ generator development was supported by FSTP project «Research in geophysical boundary layers and the development of new modelling approaches for Earth system models» within the program «Improvement of the global world-level Earth system model for research purposes and scenarios forecasting of climate change». Numerical experiments and data analysis were supported by RNF grant 24-17-00155. Stochastic Lagrangian particles model development was supported by the Russian Ministry of Science and Higher Education, agreement No. 075-15-2025-345.

Numerical experiments were carried out using the equipment of the shared research facilities of HPC computing resources at Lomonosov Moscow State University and computing resources of the Data Center of the Far Eastern Branch of the Russian Academy of Sciences.

Conflict of interests: The authors reported no potential conflict of interests.

INTRODUCTION

With the rise of urbanization, the problem of aerosol air pollution in cities has become more challenging, which has required the use of advanced modeling techniques to assess the dispersion of particulate matter in the urban environment. Understanding and being able to forecast this process is crucial for estimating health risks and developing mitigation strategies, as urban air pollution is associated with serious health consequences, including respiratory and cardiovascular diseases (Pope and Dockery 2006; Kampa and Castanas 2008; Kasimov et al. 2024). The impact of PM_{2.5} concentrations on mortality has a global effect and is especially evident in low- and middle-income countries (Cohen et al. 2017), where urbanization is usually very active.

The complexity of urban landscapes, characterized by a variety of architectural forms and types of land use, requires models with high spatial resolution to ensure effective analysis and forecasting (Baklanov et al. 2007). At the same time, processes of a wide range of scales are important for the physics of atmospheric processes in urban areas, from an individual building to a meteorological mesoscale, necessitating the use of models with different depths of process description and resolution depending on the task (Blocken 2015). Currently, there is a trend towards multi-scale modeling of meteorological processes and air pollution, as this approach allows for a more comprehensive analysis of processes and more efficient decision-making; however, it requires more complex verification of models and the development of new recommendations and standards for modeling (Kadaverugu et al. 2019; Baklanov and Zhang 2020).

Historically, aerosol dispersion modeling has relied on a Gaussian or plume approach (Berlyand 1991), which is computationally simple but does not allow for detailed consideration of the features of urban development and the underlying surface (Britter and Hanna 2003; Holmes and Morawska 2006). The development of computing technologies and computational fluid dynamics (CFD) models, primarily RANS (Reynolds-Averaged Navier-Stokes) and LES (Large Eddy Simulation) approaches, has allowed us to move to a qualitatively new level for simulation of atmospheric processes in cities. Such models reproduce the complex structure of an airflow and turbulent eddies inside urban areas (Blocken et al. 2012). The influence of urban development on microclimate and thermal comfort has been actively studied for a long time using CFD (Chatzidimitriou and Axarli 2017; Lee and Mayer 2018), but air quality is not ignored either. It has been shown that taking into account the geometry of buildings and streets has a pronounced effect on particle dispersion and allows us to obtain results that differ significantly from simulations using plume models (Oke et al. 2017). At the same time, building geometry exerts complex nonlinear effects on particle concentrations (Starchenko et al. 2023) and provides notable impact on other components of the urban environment, including the air quality, e.g., via greening of roofs (Wu and Liu 2023; Venter et al. 2024).

One of the methods to tackle the issues listed above is the use of LES models, since with sufficient computing resources they can provide a more accurate representation of air flows and turbulence in urban areas than the more popular RANS models (Zheng and Yang 2021). This approach is already used for real urban development on the scale of an entire city and allows us to draw conclusions about the influence of street orientation on the dispersion of pollutants (Zhang et al. 2021). In addition, LES models are

used to verify simpler models or parameterizations used for operational forecasting of air quality and atmospheric composition (Grylls et al. 2019). Of particular interest are studies using LES models with Lagrangian tracking of pollutants as individual particles (Glazunov 2018), which accounts for the interaction of solid particles with the urban atmosphere and buildings in a more explicit way compared to Eulerian models; e.g., this approach was used to assess the impact of building development and atmospheric stratification on particle dispersion in Helsinki (Kurppa et al. 2018).

An important achievement in the field of urban meteorology is the creation of the concept of local climate zones (LCZ) and its use in hydrodynamic models of various scales. LCZ classifies urban areas based on building and street parameters, vegetation cover, and surface properties - these variables strongly affect the local microclimate and the structure of air flows (Stewart and Oke 2012). Studies using the LCZ classification are primarily focused on quantifying urban morphology impact on air or surface temperature (Varentsov and Samsonov 2020; Aslam and Rana 2022), however, there are more and more works on the topic of air quality, which demonstrate that the characteristics of urban development strongly affect the concentrations and surface deposition of pollutants (Kosheleva et al. 2018), and many classifications of the underlying surface are not relevant to urban morphology, which is presented in the LCZ (Jiang et al. 2023). It has been repeatedly shown that there is a relationship between the LCZ types and the concentration patterns of solid particles (Shi et al. 2019; Lin et al. 2024; Nourani et al. 2024), however, conclusions about the specific nature of this relationship vary depending on the city and research methods.

The aim of this study is to apply a novel approach combining Large Eddy Simulation with Local Climate Zones classification to analyze the impact of urban development geometry on air pollution at various scales, from district level to individual buildings. This approach not only deepens our understanding of atmospheric environment dynamics in urban settings but also paves the way towards projecting more resilient urban infrastructures and healthier living environments.

MATERIALS AND METHODS

Large Eddy Simulation

As the main tool, we used the model developed at the RCC MSU (Lomonosov Moscow State University Research Computing Center) and the INM RAS (G.I. Marchuk Institute of Numerical Mathematics of the Russian Academy of Sciences) based on a unified hydrodynamic code combining LES (Large Eddy Simulation), DNS (Direct Numerical Simulation) and RANS (Reynolds Averaged Navier-Stokes) approaches for modeling geophysical turbulent flows with high spatial resolution (Mortikov et al. 2019; Kadantsev et al. 2021; Tkachenko et al. 2022; Debolskiy et al. 2023, Suiazova et al. 2024). In this work, the LES configuration of the model was used, which allows for a detailed reproduction of turbulent airflows in the presence of complex urban geometry.

This model calculates the dynamics of a thermally stratified fluid defined using filtered Navier-Stokes equations in the Boussinesq approximation. To parameterize the subgrid stress tensor, the Smagorinsky eddy viscosity model is used, in which the Smagorinsky constant and the subgrid Prandtl number (which depend on time and spatial coordinates) are determined using a dynamical procedure (Germano et al. 1991). The numerical

model utilizes conservative finite-difference schemes of second-order accuracy for spatial approximation on rectangular meshes. A fractional step method is used to integrate the equations of motion and continuity over time and to ensure the incompressibility condition, and an explicit third-order Adams-Bashforth scheme is used to approximate the momentum and heat equations.

An important feature of this model is explicit representation of the buildings (Tarasova et al. 2024). The surface of buildings can be given its roughness and temperature, which allows us to make simulations including complex scenarios when different buildings have different properties.

Lagrangian particle model

To model particulate matter transport in the urban atmosphere, a Lagrangian particle transport module was introduced to the LES model. The main advantage of the Lagrangian approach is its ability to track the trajectories of individual particles in detail, which allows explicitly describing their interaction with the diverse elements of the urban environment. In complex urban environments where buildings, streets, and green spaces create heterogeneous airflow patterns, the Lagrangian method can account for the effects of turbulence, particle sedimentation on buildings surfaces, and changing atmospheric conditions near surfaces, resulting in more accurate predictions of local concentrations compared to the Eulerian framework.

In this paper, the Lagrangian approach is used for numerical modeling of aerosol transport. Each particle is tracked through its entire trajectory, as well as the particle's velocity and other state variables. This approach is used to track a limited number of particles but allows us to explicitly consider the forces acting on the particle. Using the Lagrangian approach, the change in position of each individual particle is described by the Eq. (1) (Thomson and Wilson 2012):

$$dx_p = u_p dt \quad (1)$$

where x_p – particle position, u_p – its velocity, t – time. The developed model allows to consider inertial (“heavy”) particles, whose velocity may not coincide with the velocity of the ambient air at particle position. Therefore, changes of both particle's position and its velocity have to be calculated – Eq. (1) is supplemented with Eq. (2) for velocity based on Newton's second law:

$$\frac{du_p}{dt} = \frac{g(\rho_p - \rho)}{\rho_p} + F_D(u - u_p) \quad (2)$$

where $g=(0,0,-g)$ – gravitational acceleration ($g>0$) in Cartesian coordinates, ρ_p – particle density, ρ – air (medium) density, $u=(u_x, u_y, u_z)$ – ambient flow (medium) velocity, F_D – drag coefficient.

To account for the interaction with buildings, parameterization of collisions with hard (impermeable) surfaces has been implemented, in which both reflection of a particle from the surface of a building and deposition on it are possible. It is implemented by representing buildings as impenetrable surfaces of the computational grid.

The Lagrangian transport module also takes into account the effect on particle motion of the turbulent eddies which are subgrid for LES model. The total flow velocity from Eq. (2) is represented as the sum of the averaged and subgrid components (Eq. 3):

$$u = \bar{u} + u' \quad (3)$$

where \bar{u} – velocity explicitly resolved at the numerical grid of LES model, u' – subgrid velocity fluctuation which is evaluated using the Lagrangian stochastic model (LSM). The 1st order LSM is used in this work, for which the change of fluctuation component along the trajectory of a fluid parcel (coinciding with the particle path for light particles) can be calculated as Eq. (4) (Reynolds and Cohen 2002):

$$du'_i = -\frac{1}{2}b^2 \frac{u'_i}{\sigma_{u_i}^2} dt + b\xi_i \quad (4)$$

where $i=1,2,3$ is the Cartesian coordinate index, $b^2=C_0\varepsilon$, $\sigma_{u_i}^2$ – subgrid velocity variance, $C_0=6.0$ – Kolmogorov's constant, ε – the rate of dissipation of turbulent kinetic energy, diagnosed by LES model, ξ_i – independent delta-correlated (in time) Gaussian random variables with standard deviation $\sigma_{\xi_i} = \sqrt{dt}$.

The developed Lagrangian transport module was previously verified on analytical solutions for light and heavy particles (Varentsov et al. 2020; Varentsov et al. 2023).

Urban configurations

Since a limited number of numerical experiments cannot cover the entirety of urban geometry variability, to select urban geometry configurations for LES experiments, it was necessary to choose building development types that are both idealized enough to be described by a small set of properties and easily reproduced in other studies and relevant to the real urban settings so that they could describe urban areas in different cities of Russia and the world. The classification of Local Climate Zones (LCZ), proposed in (Stewart and Oke 2012), is increasingly used as such a universal tool for identifying characteristic types of homogeneous (in terms of mean morphological characteristics) urban development within a city.

We restrict our study to 3 types of LCZ – the selected configurations are LCZ 4, LCZ 5, and LCZ 6. The parameters defining each type are shown in Table 1. These types of LCZ are widespread both in Russia and in the world, as evidenced by the global LCZ map (Demuzere et al. 2022). Configurations LCZ 1, LCZ 2, LCZ 3, and LCZ 7 require calculations with more detailed resolution and higher computational cost due to the very high density of buildings, and LCZ 8, LCZ 9, and LCZ 10 are not so common in residential areas of Russian cities – so these types are planned to be considered not now, but in further studies.

LCZ 4 is an open high-rise building zone. In Russian cities, a common example of such development is Soviet-era housing, which typically consists of tower blocks with 8 to 12 floors in park-like surroundings. LCZ 5 is an open medium-rise building zone. The typical example is the neighborhoods of Soviet five-storey apartment buildings (e.g., so-called “khrushhevka”), typical of almost any Russian city. LCZ 6 is an open low-rise building zone, and it can include areas with both individual private houses and low-rise apartment buildings. Common examples in Russia are suburbs with private houses and city districts built up with two-storey communal housing.

To generate building geometry so that the whole domain corresponds to one of the selected LCZs, two methods were used: manual specification of the geometry with a regular pattern and automatic generation of the geometry with a randomized pattern using specially developed generator software. Hereafter, the

Table 1. LCZ parameters used to generate the building geometries for numerical experiments

LCZ	Buildings height	Building areal fraction	Aspect ratio (the ratio of building height to street width)
LCZ 4	> 25 m	20-40 %	0.75-1.25
LCZ 5	10-25 m	20-40 %	0.3-0.75
LCZ 6	3-10 m	20-40 %	0.3-0.75

configurations of these two types are called “regular” and “randomized”, respectively.

As a result of the manual generation of regular geometry, 9 configurations were prepared (Fig. 1), with 3 variants for each of the selected LCZ. The only differences between the LCZs in these configurations were building height and aspect ratio, while the shape and orientation of the buildings differed between LCZ variants. The first two options (LCZ 4 (a-b), LCZ 5 (a-b), LCZ 6 (a-b)) are regular patterns with long buildings forming urban canyons stretching from South to North or from West to East, such scenarios mimic areas of Soviet residential districts, newly built according to the cities’ master plans (Engel 2022). The third option (LCZ 4 (c), LCZ 5 (c), LCZ 6 (c)) is the regular pattern of square buildings, typical for some urban areas of the 21st century in Russia and for many cities around the world, especially in developing countries.

Urban development rarely has a perfectly periodic structure, so the regular geometry of identical buildings and streets presented above is an idealized option. A pseudorandom pattern of buildings of similar scale can be found in almost any city. To consider more realistic scenarios, we have created randomized building geometries in which the structure of streets, blocks, and buildings is present, but their location and parameters are random within acceptable values for a particular LCZ.

The approach of generating building geometry based on specified characteristics is used both in atmospheric flow simulations in general (Sutzi et al. 2020) and specifically

for LCZ classification (Zhou et al. 2023). However, the available generation methods are usually limited in setting or selecting parameters. Therefore, to generate a randomized building geometry, we developed a generator tool that takes as input the area size and the morphological characteristics of the selected LCZ, including parameters from Table 1 and manually selected restrictions on building sizes. Next, the fractal geometry of urban development is generated in several stages.

At the first stage, the minimum and maximum sizes of streets and blocks and their number are calculated based on the LCZ parameters. The area is randomly divided into a corresponding number of streets (along the X and Y axes) and rectangular blocks; all random values have a uniform distribution within the minimum and maximum sizes mentioned above. A block refers to an area with a width of 1 to 3 buildings and a length of at least 1 building. At the second stage, rectangular building objects are generated in each of the obtained blocks, taking into account the LCZ parameters and the selected building size restrictions. The third stage of the generation is to check the correspondence of the generated geometry and the selected LCZ. The morphological characteristics (height and area of buildings, aspect ratio) are checked separately for each block. If any of the parameters deviate by more than 5% from the required value, the buildings in this block are generated again. If in a certain quarter it is not possible to achieve the required values in several generation attempts, or all blocks are approved, but a deviation of more than 5%

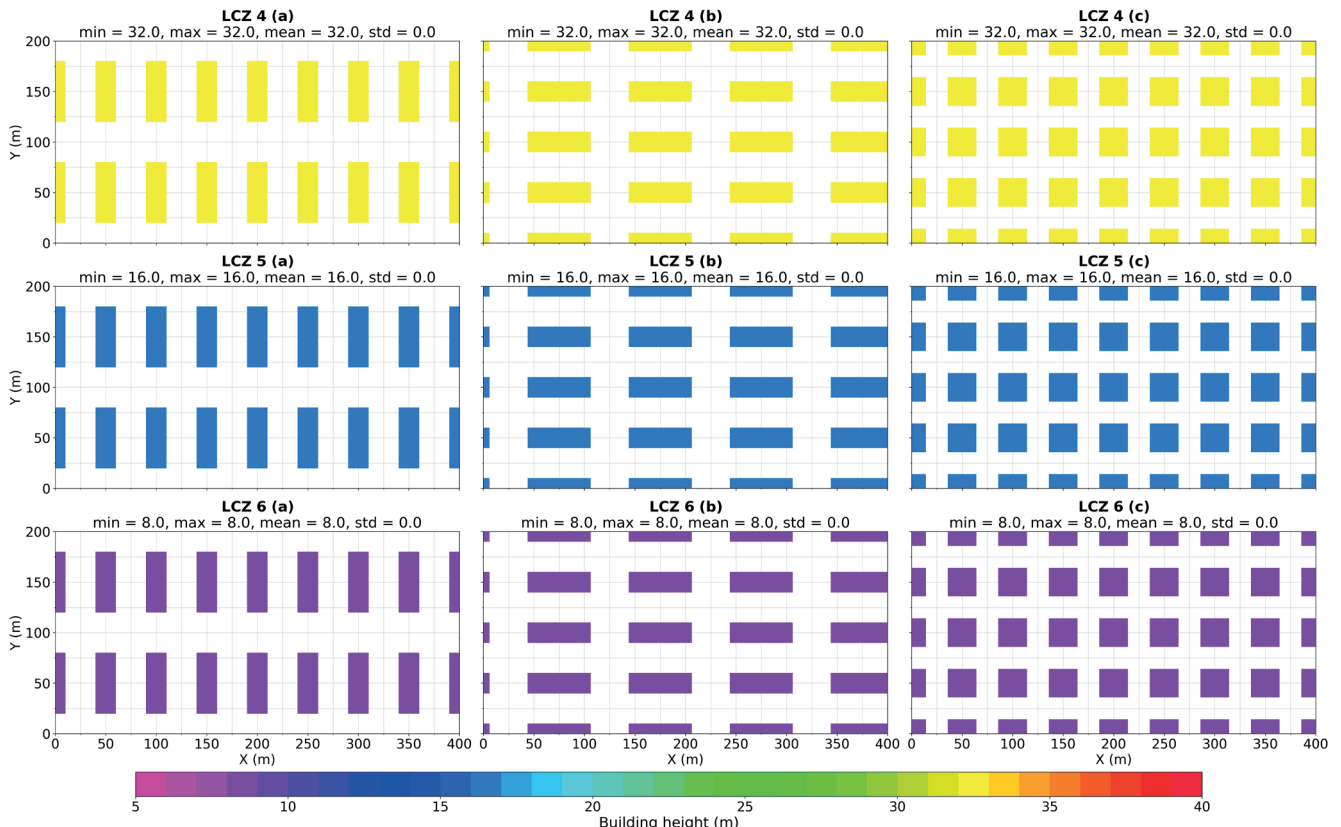


Fig. 1. Elevation maps for manually created regular building configurations corresponding to Local Climate Zones LCZ 4, LCZ 5, and LCZ 6

is obtained for the entire region, then the entire region is being regenerated, that is, streets and blocks.

In this way, 12 building configurations were generated, 4 for each LCZ (Fig. 2). The main differences between randomized and regular configurations are the variation in building sizes and heights, the different shape and orientation of buildings within even one block, the lack of a regular structure, and the different number and width of streets. The building sizes for LCZ 4 and LCZ 5 are quite similar for both generation methods. However, the randomized LCZ 6 configurations have significantly more buildings, and their size is smaller than in the regular LCZ 6 configurations, which is caused by the limitations of the generation method.

Although such a random building pattern may not have exact real-world analogues, it can be called more realistic, since perfectly regular geometry is extremely rare in cities (even cities built according to master plans usually have a heterogeneous structure), and randomized buildings of the same scale can be found in almost any city.

Numerical experiments setup

For each building configuration (for 9 regular and 12 randomized ones), a numerical experiment was conducted to compute aerosol transport. The experiments simulated

the spread of atmospheric pollutants emitted from the street in the form of vehicle emissions and fine road dust. The spread of such pollutants within urban areas was assessed under common meteorological conditions: low wind and neutral atmospheric stratification, which together provide ventilation of the city and vertical mixing, but with low intensity.

The characteristic meteorological conditions of the experiments included the wind speed and direction at the upper boundary, as well as the vertical temperature gradient. The wind boundary conditions were set to 4 m/s at an altitude of 120 m and above, and the wind direction was westerly (along X-axis). For temperature, the boundary conditions were set to +15 °C at an altitude of 120 m and +16 °C on the surface of the earth and buildings, which ensured neutral temperature stratification of the atmosphere when vertical air mixing, unlike stable stratification, is significant but not as active as with unstable stratification. The lateral boundaries were set with periodic conditions for atmospheric parameters, allowing the airflow to be adapted to the geometry of urban development as if a similar pattern of buildings surrounded the entire domain area. The graphical representation of the experiment setup is shown in Fig. 3.

Spherical solid particles with a diameter of 1 μm and a material density of 1000 kg/m³ were defined as

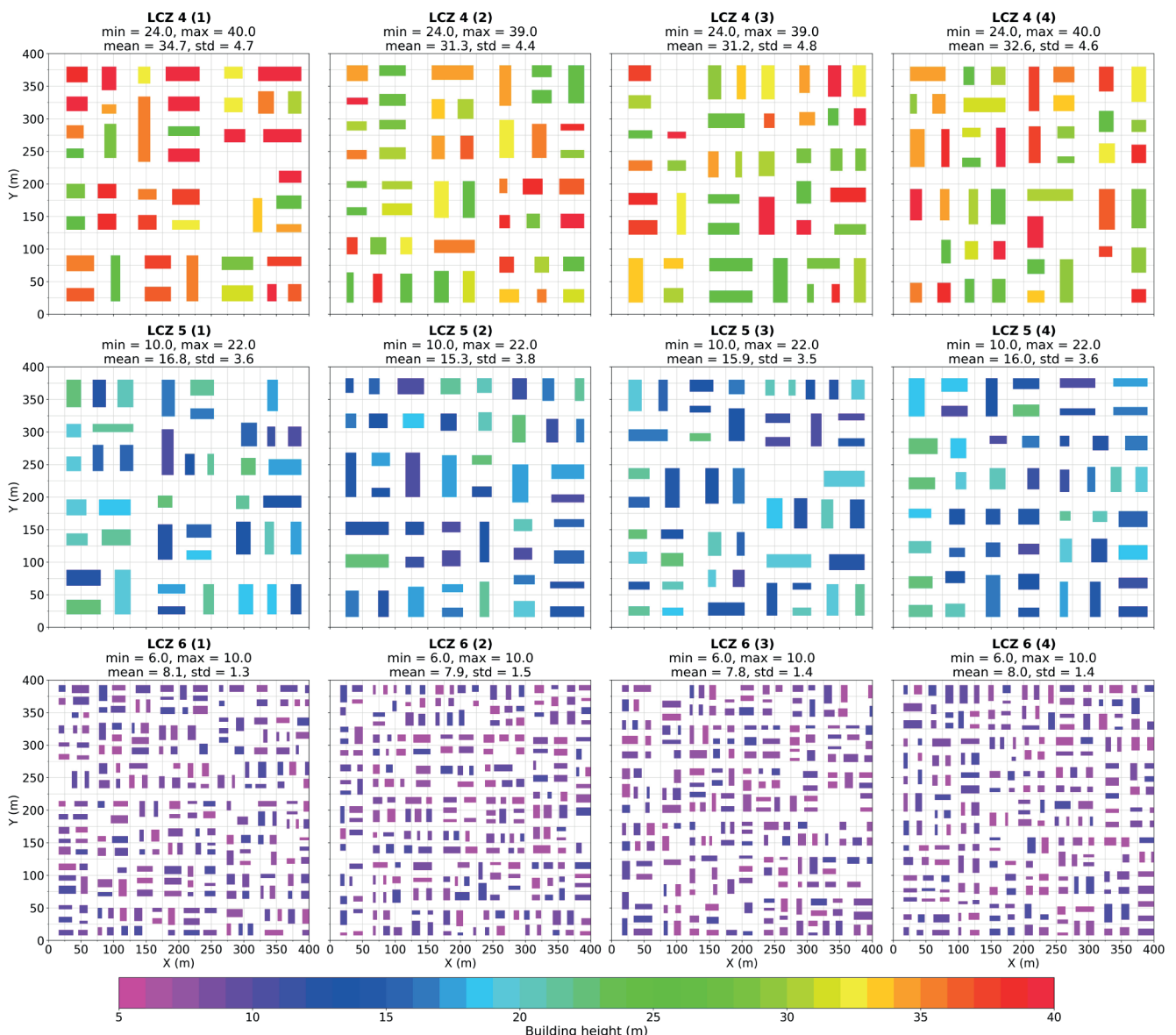


Fig. 2. Elevation maps for randomized building configurations corresponding to Local Climate Zones LCZ 4, LCZ 5, and LCZ 6

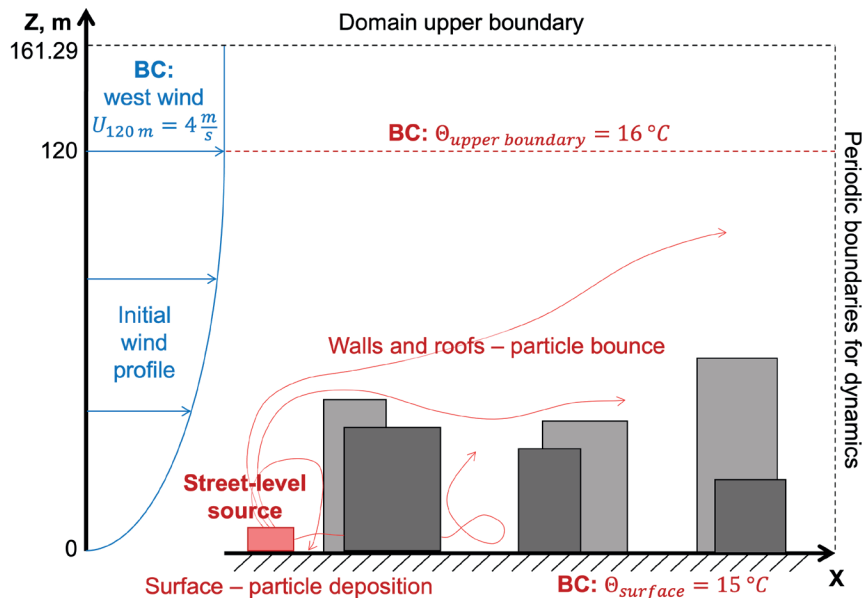


Fig. 3. Schematic of the experiment setup

aerosols, which correspond to the widely used aerosol category PM_{2.5} (Zwozdziak et al. 2017). The particles we are considering are relatively light and weakly affected by inertia and gravitational subsidence. Heavier and larger particles (PM₁₀ and larger) are planned to be considered in future studies. The source of particles in all experiments was a volumetric source having a width of 8 meters (along X) and a height of 4 meters (from 0 to 4 m along Z) and elongated through the entire Y axis, that is, simulating emissions from a long street perpendicular to the wind direction. In configurations with regular geometry, the source was located at coordinates from X=21.0 to X=29.0 meters from the western border of the domain; that is, it was located in the first left canyon. In configurations with randomly generated geometry, the source occupied the south-north strip at coordinates from X=4.0 to X=12.0 meters, i.e., it was also located in the first left canyon. Particles escaped domain on the western, eastern, and upper borders of the computational domain, periodic conditions were set on the southern and northern borders (particles appear at the southern margin while crossing the northern, and vice versa), and deposited on the earth's surface.

The dimensions of the computational domain were 400 (X) m by 200 (Y) m by 161.29 (Z) m for regular configurations and 400 (X) m by 400 (Y) m by 161.29 (Z) m for randomized ones. The horizontal grid spacing along the X and Y axes was 2 m, the vertical resolution was 2 m inside bottom 80-meter layer, and above it the cell size increased by 4% with each grid step up to 5.12 m. In total, the vertical domain extent was divided into 64 cells. The experiments were carried out for a period of 12 hours, sufficient for the flow to achieve a quasi-stationary equilibrium state and gather statistics (mean and fluxes) in the last 4 hours of the simulation. The time step of the LES model was fixed in all cases and equal to 0.04 seconds.

RESULTS AND DISCUSSION

Regular configurations

Based on the results of numerical experiments, the distribution of particle concentrations and the characteristics of their propagation were analyzed. For regular building configurations, Fig. 4 shows the average concentrations at the ground level (0-4 m above surface), demonstrating the removal of particles from the source

through the streets. In the plots of time-averaged near-surface concentrations, plumes of higher concentrations can be clearly traced along the streets through which the particles are carried horizontally. The maximum average concentrations are observed in LCZ 4 (a-c), which can be explained by the highest height of buildings among the selected LCZs and, as a result, the greatest resistance to airflow, which negatively affects the street ventilation. At the same time, there is no significant difference in average concentrations and standard deviation (SD) of concentrations between LCZ 5 (a-c) and LCZ 6 (a-c), despite the twofold difference in the height of buildings.

Significant differences are noticeable among the various building configurations that belong to the same LCZ (between (a), (b) and (c) configurations of each same LCZ). For each of the LCZs, it can be seen that the lowest concentrations were obtained in configuration (a), elongated buildings perpendicular to the wind, which is associated with the formation of vertical vortices (Glazunov 2018) inside the canyons and the active removal of particles into the layer above the buildings. At the same time, configurations (b) show average concentrations that are 10-15% higher, which is associated with a lower vertical mixing effect and a more active removal of particles along the streets at the same height near the surface. The highest average concentrations and SD are observed in configurations (c) – these are the variants with the highest building density, which affects the weakening of vertical mixing and a decrease in wind speed inside the urban canopy.

Randomized configurations

For randomly generated configurations, the average concentrations at the ground level (0-4 m in height) are shown in Fig. 5. Due to the random nature of the building patterns, there are much more significant differences between LCZs and, as before, noticeable differences between realizations of a single LCZ. The most noticeable difference from the experiments with regular configurations (Fig. 4) is that the highest average concentrations were obtained for LCZ 6 with the lowest building height, while the values for LCZ 4 and LCZ 5 are similar. Such a drastic difference can be explained by the fact that in the case of randomized geometry, the airflow becomes more turbulent, and the role of vertical mixing

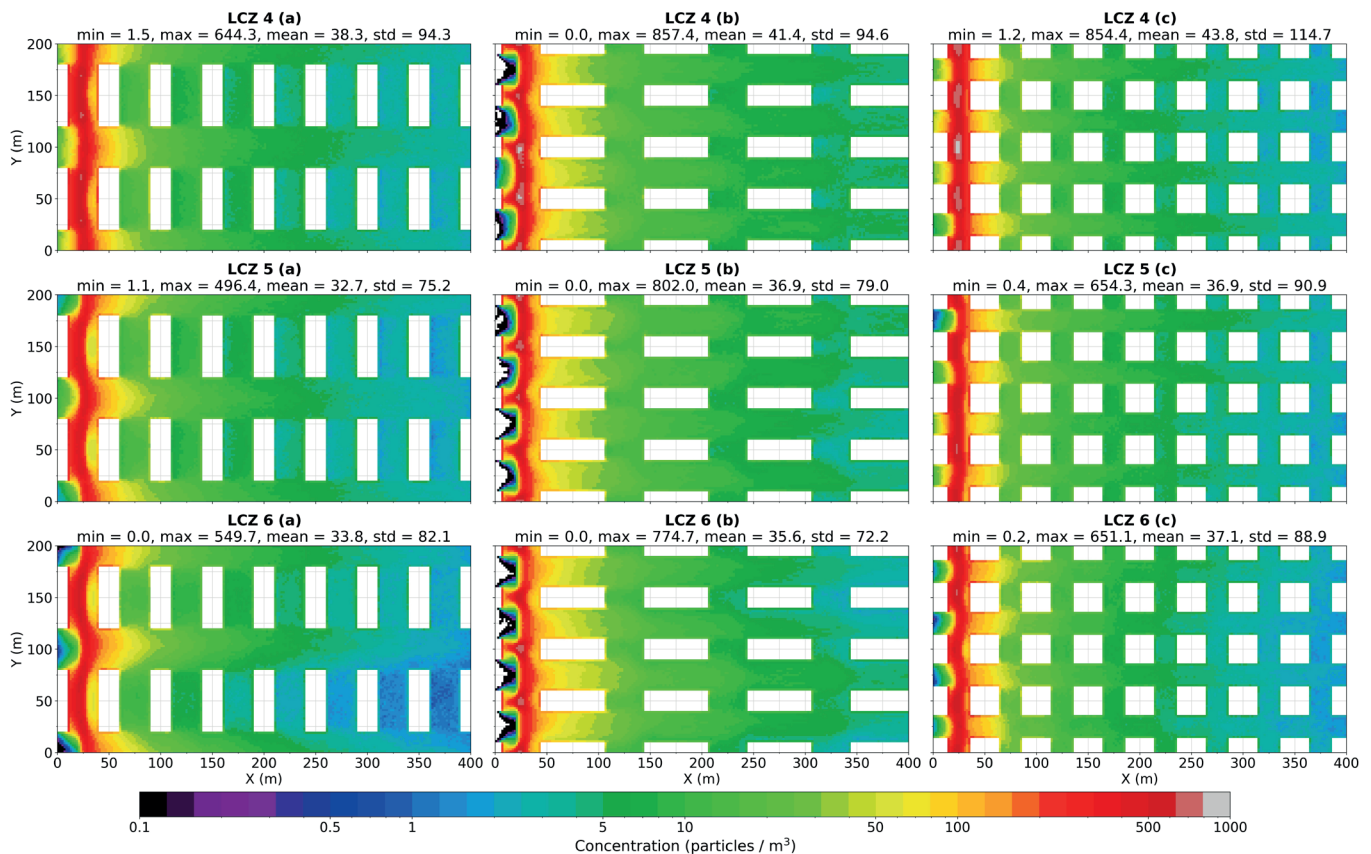


Fig. 4. Simulated surface (altitude 0-4 m) particle concentrations for regular building configurations corresponding to Local Climate Zones LCZ 4, LCZ 5, LCZ 6

and removal of particles into the air layer above buildings increases. At the same time, in the case of LCZ 6, the urban environment is lower and denser than in LCZ 4 and LCZ 5. This, in turn, reduces the exchange between the air layers inside it and above the buildings.

If we compare different configurations within the same LCZ, then there is a very strong influence of geometry near the source – concentrations at different points at the same distance from the source may differ by an order of magnitude, but at large enough distances, this is smoothed out due to the random nature of the urban development.

From the above results, it can be concluded that buildings parallel to the wind (regular configurations (b), Fig. 4) contribute to the horizontal removal of particles without active vertical mixing, while perpendicular buildings (regular configurations (a), Fig. 4) contribute to the vertical removal of air into the layer above buildings. However, these effects have been tested under conditions of neutral stratification. In cities with frequent stable stratification, i.e., at high latitudes and in winter (Varentsov et al. 2023), the removal of aerosols requires the presence of well-ventilated streets and courtyards. With frequent daytime unstable stratification, particle removal will also be accelerated by wind-obstructing structures that activate vertical mixing. However, from the point of view of aerosol removal, randomized building configurations have been proven to be the best, in which streets parallel to the wind and buildings perpendicular to the wind are combined, but low building density remains – in total, all this leads to increased turbulence and active horizontal and vertical mixing.

Configurations intercomparison

To assess the LCZ classification relevance to pollution dispersion in urban environments, we determined how large the differences in concentration and particle transport patterns are between variations in geometry within a single LCZ type.

Fig. 6 shows vertical profiles of particle concentrations averaged over the eastern half of the region (coordinates [200:400 m, 0:400 m] on the X and Y axis respectively), that is, over the part of the building as far away from the sources as possible, where the concentration field is already significantly mixed by buildings and less dependent on the position of buildings compared to the latter located directly next to the source. The general shape of the profiles is similar for most configurations. The maximum concentrations are observed at a height close to the average building height, since inside the urban canopy, vertical mixing lifts particles up, but above the roofs, it is not so active, and particles are carried away by horizontal flows. At the same time, particles sediment on the ground, so surface concentrations are not high at a distance from the source. For some configurations, high concentrations are observed not only at the roof level but also up to the upper boundary of the domain. This effect can be caused by the severe turbulence that occurs over tall and highly heterogeneous urban development.

For regular geometries (Fig. 6a, 6c, 6e), the profiles and the spread between them are very similar – the standard deviation of concentration ranges from 0.23 to 0.27 (in dimensionless units relative to the maximum concentration among the profiles), and the shape of the profiles for the same buildings' configurations but for different LCZs is the same (with profiles normalized by building heights), e.g., for (c) configurations of all LCZs. For each of the LCZs, there is a large variation in concentrations between different versions of its geometry, which suggests that the LCZ cannot be approximated by any single geometry configuration – it is necessary to consider various options and take into account the influence of the shape and orientation of buildings.

For randomized geometries, similar conclusions were obtained for LCZ 4 and LCZ 5 (Fig. 6b, 6d) – the profiles for different configurations of the same LCZ differ significantly from each other. However, for LCZ 6 (Fig. 6f), extremely low variability was obtained between the geometry variants – due

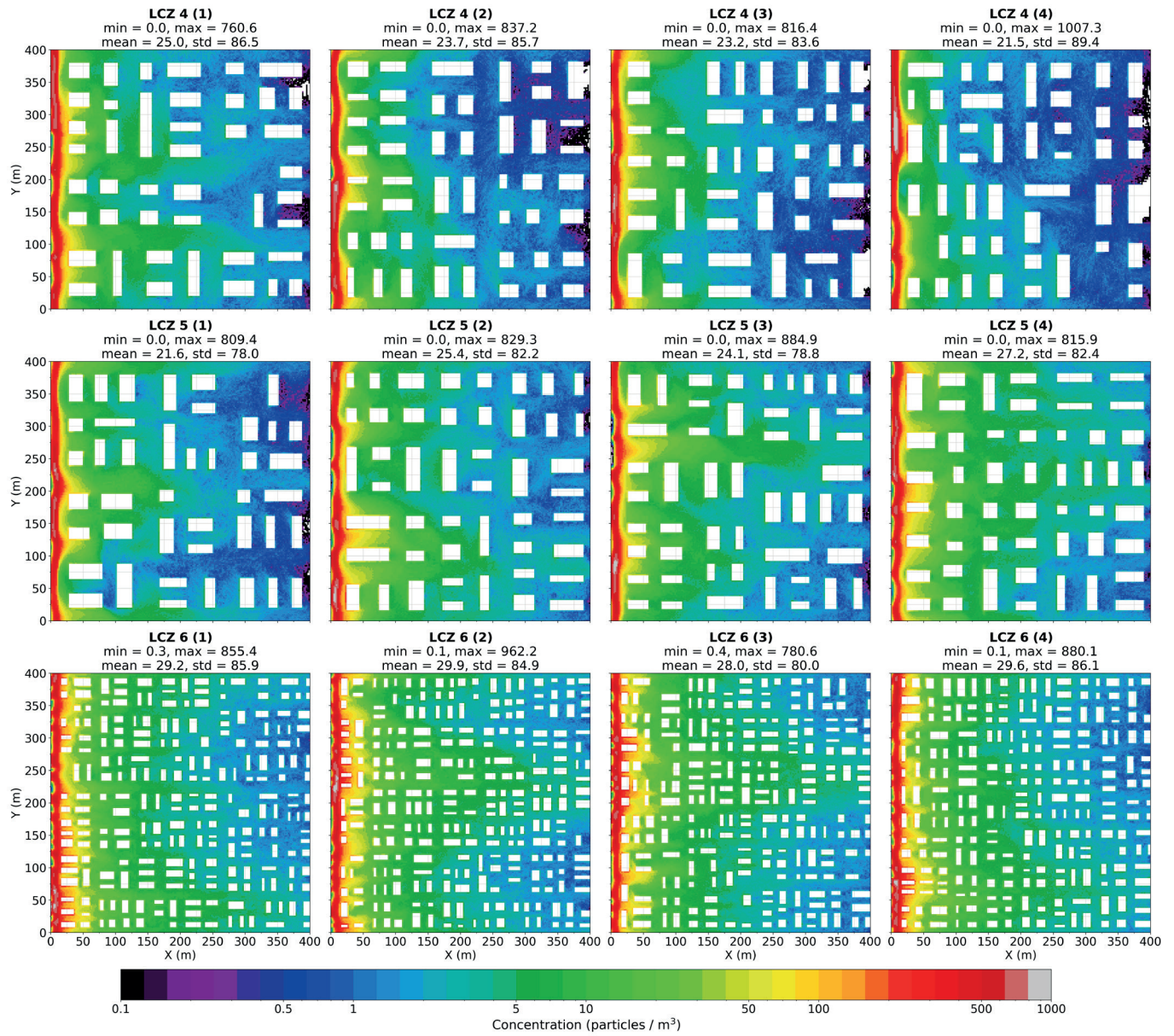
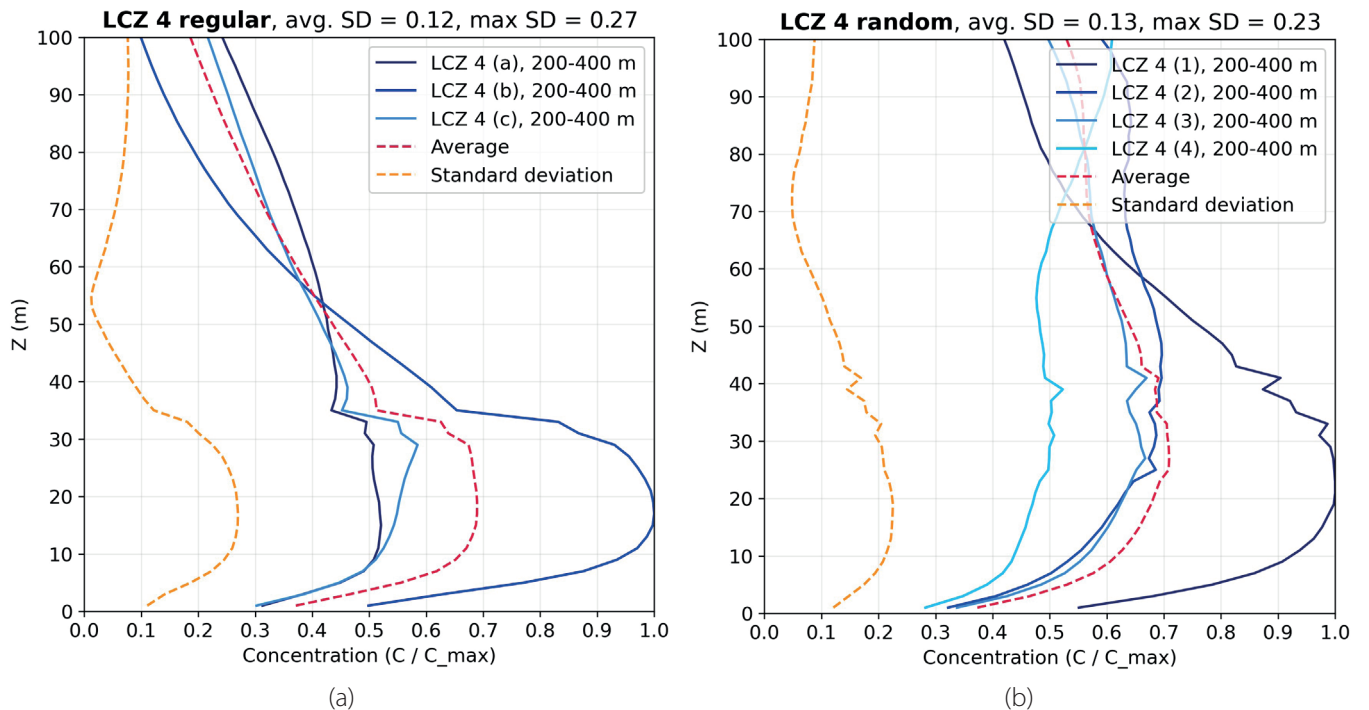


Fig. 5. Simulated surface (altitude 0-4 m) particle concentrations for randomized building configurations corresponding to Local Climate Zones LCZ 4, LCZ 5, LCZ 6



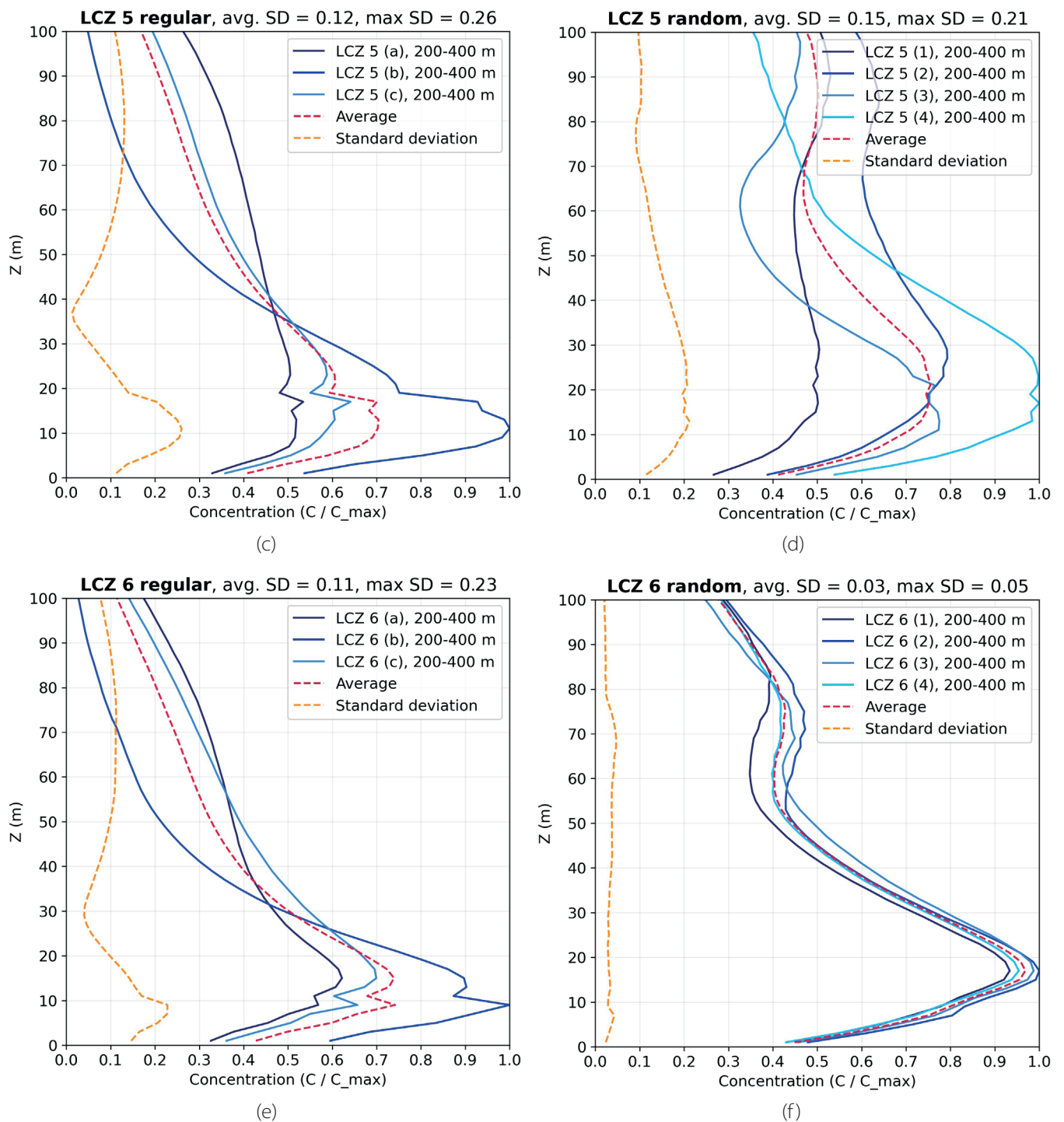


Fig. 6. Vertical particle concentration profiles, averaged over the eastern half of the region, for regular (a, c, e) and randomized (b, d, f) building configurations corresponding to Local Climate Zones LCZ 4 (a-b), LCZ 5 (c-d), LCZ 6 (e-f)

to the low height and small size of the buildings, unlike LCZ 6 regular configurations with longer and wider buildings, the geometry of buildings is more homogeneous and does not generate large disturbances in the wind flow.

Fig. 7 shows concentration profiles similar to Fig. 6, but averaged over all configurations of the same LCZ. In the case of regular geometries (Fig. 7a), the difference between different LCZ types is minimal at the surface and only significantly manifests itself at the roof level and in the layer above the buildings. The maximum standard deviation (0.2) turned out to be less than when comparing different geometry configurations within a single LCZ. Thus, for regular building configurations, the shape and orientation of buildings had a greater impact on the spread of aerosols than the different LCZ parameters: the height of the building and the aspect ratio of urban canyons.

For the randomized configurations (Fig. 7b), on the contrary, significant differences were found between the profiles for different LCZs. The maximum standard deviation values observed at heights of 15–20 m were approximately 1.5 times higher than the maximum standard deviation values for various configurations within the same LCZ. The average concentrations also vary significantly at the surface level – for LCZ 6, they were almost 2.5 times higher than for LCZ 4. The results for the randomized configurations demonstrate that in the absence of an ideal periodic structure of the city and the presence of heterogeneity in the size, shape, and height of buildings, the spread of aerosols in the urban environment is determined by the general morphometric parameters of the area much more strongly than the specific location of buildings and their orientation.

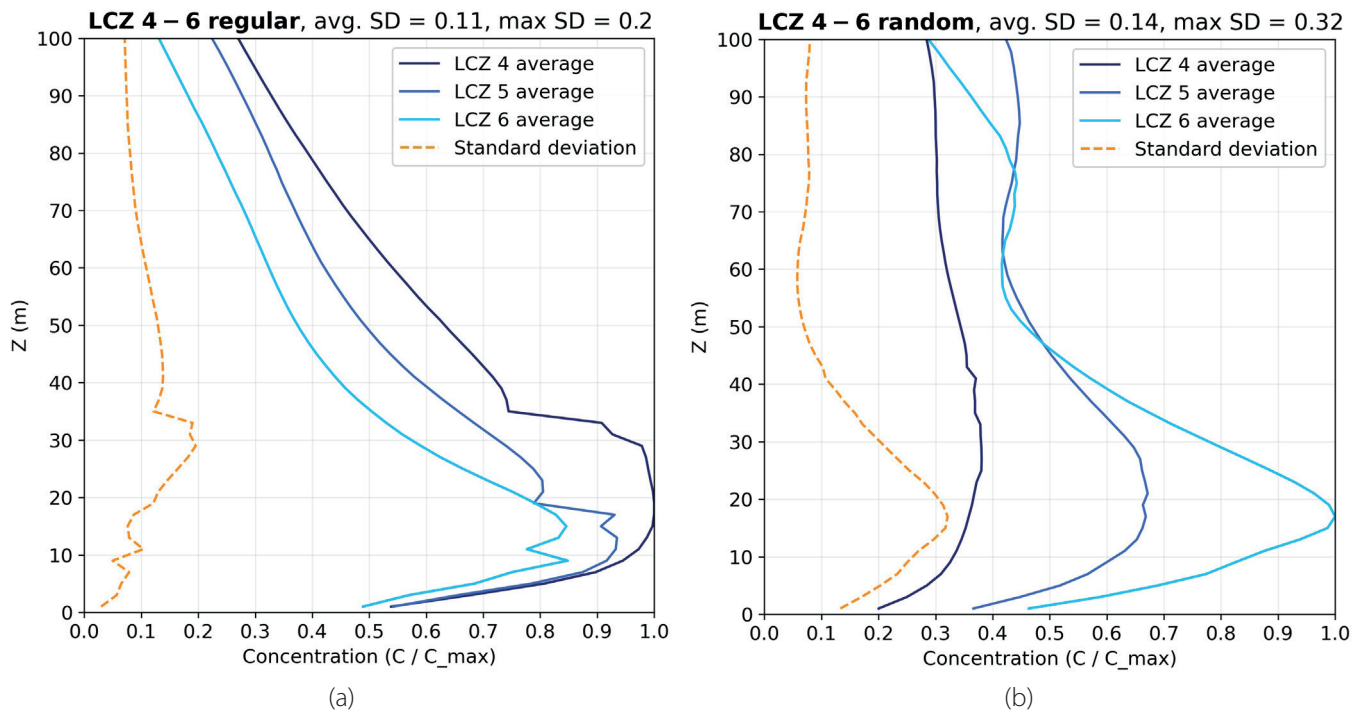


Fig. 7. Vertical particle concentration profiles in the eastern half of the region averaged over the implementations of each LCZ, for regular (a) and randomized (b) building configurations

CONCLUSIONS

In this paper, the analysis and comparison of aerosol particle dispersion within the city were carried out depending on the following parameters. Firstly, depending on the type of urban development based on the LCZ classification. Secondly, depending on the specifics of the geometry implementation for the selected LCZ type. Thirdly, depending on the randomization and periodicity of the geometry configuration. The results of numerical calculations using a large-eddy simulation model with a Lagrangian particle transport model allowed us to draw conclusions for a finely dispersed urban aerosol distribution under typical meteorological conditions: neutral stratification and low wind.

When generating regular geometry with identical buildings, the influence of the features of a particular configuration (primarily, the shape and orientation of buildings) turned out to be comparable, and in some cases more significant, than the influence of large-scale morphometric parameters of buildings, which are determined by LCZ types and characterize qualitatively different types of urban development. However, such LCZ implementations are highly idealized and have very few analogues in real cities, which motivates the creation of configurations with a limited range of building parameters and a random contribution to their location relative to each other.

Using the developed LCZ generator, building configurations were created taking into account the random contribution to the parameters and location of each building but corresponding to the large-scale morphometric characteristics of the selected LCZ types. Such configurations are more realistic, as they reflect the quasi-random nature of real urban development at the level of individual buildings but retain the typical

scale of blocks and streets for most cities. Experiments with these configurations showed a significant variation in concentrations between specific implementations of a single LCZ for high-rise and medium-rise buildings (LCZ 4, LCZ 5) and a slight variation for low-rise buildings (LCZ 6), while for all LCZs the scale of variation between implementations was smaller than in the case of regular configurations. The differences between LCZs in this case turned out to be one and a half times greater than the maximum scale of differences between individual implementations of a single LCZ.

Thus, in urban areas, which are highly distinct from the single, regular, periodic structures, it is possible to describe the features of aerosol distribution by considering the aggregated type of urban development – for example, the LCZ type. This result opens up new prospects for the development of global and regional models of atmospheric dynamics and pollution dispersion by more accurately accounting for the urban underlying surface and its effect on the spread of aerosols.

Based on the results of this work, the following recommendations can be proposed for developers and urban planners. With low and medium building densities, one of the ways to increase air mixing and remove polluting aerosols from the surface level may be to increase the height spread of buildings and make their location and orientation more random, avoiding the construction of identical regular structures.

Further research on this topic is required to analyze the differences more accurately between all existing types of LCZ and to take into account a larger number of factors: atmospheric stratification, wind speed, aerosol size and composition, interaction of different LCZ types on the city scale, etc. Also, in further research, it is worth considering in more detail the influence of model parameters, especially spatial resolution. ■

REFERENCES

- Aslam A. and Rana I.A. (2022). The use of local climate zones in the urban environment: A systematic review of data sources, methods, and themes. *Urban Climate*, 42, 101120. DOI: 10.1016/j.uclim.2022.101120
- Baklanov A., Hänninen O., Slørdal L.H., Kukkonen J., Bjergene N., Fay B., Finardi S., Hoe S.C., Jantunen M., Karppinen A., Rasmussen A., Skouloudis A., Sokhi R.S., Sørensen J.H. and Ødegaard V. (2007). Integrated systems for forecasting urban meteorology, air pollution and population exposure. *Atmospheric Chemistry and Physics*, 7(3), 855–874. DOI: 10.5194/acp-7-855-2007
- Baklanov Alexander and Zhang Y. (2020). Advances in air quality modeling and forecasting. *Global Transitions*, 2, 261–270. DOI: 10.1016/j.glt.2020.11.001
- Berlyand M.E. (1991). *Prediction and Regulation of Air Pollution*. Springer Netherlands. DOI: 10.1007/978-94-011-3768-3
- Blocken B., Janssen W.D. and van Hooff T. (2012). CFD simulation for pedestrian wind comfort and wind safety in urban areas: General decision framework and case study for the Eindhoven University campus. *Environmental Modelling & Software*, 30, 15–34. DOI: 10.1016/j.envsoft.2011.11.009
- Blocken Bert. (2015). Computational Fluid Dynamics for urban physics: Importance, scales, possibilities, limitations and ten tips and tricks towards accurate and reliable simulations. *Building and Environment*, 91, 219–245. DOI: 10.1016/j.buildenv.2015.02.015
- Britter R.E. and Hanna S.R. (2003). Better lowercase: Flow and dispersion in urban areas. *Annual Review of Fluid Mechanics*, 35(Volume 35, 2003), 469–496. DOI: 10.1146/annurev.fluid.35.101101.161147
- Chatzidimitriou A. and Axarli K. (2017). Street Canyon Geometry Effects on Microclimate and Comfort; A Case Study in Thessaloniki. *Procedia Environmental Sciences*, 38, 643–650. DOI: 10.1016/j.proenv.2017.03.144
- Cohen A.J., Brauer M., Burnett R., Anderson H.R., Frostad J., Estep K., Balakrishnan K., Brunekreef B., Dandona L., Dandona R., Feigin V., Freedman G., Hubbell B., Jobling A., Kan H., Knibbs L., Liu Y., Martin R., Morawska L., ... Forouzanfar M.H. (2017). Estimates and 25-year trends of the global burden of disease attributable to ambient air pollution: an analysis of data from the Global Burden of Diseases Study 2015. *The Lancet*, 389(10082), 1907–1918. DOI: 10.1016/S0140-6736(17)30505-6
- Debolskiy A.V., Mortikov E.V., Glazunov A.V. and Lüpkes C. (2023). Evaluation of Surface Layer Stability Functions and Their Extension to First Order Turbulent Closures for Weakly and Strongly Stratified Stable Boundary Layer. *Boundary-Layer Meteorology*, 187(1–2), 73–93. DOI: 10.1007/s10546-023-00784-3
- Demuzere M., Kittner J., Martilli A., Mills G., Moede C., Stewart I.D., Van Vliet J. and Bechtel B. (2022). A global map of local climate zones to support earth system modelling and urban-scale environmental science. *Earth System Science Data*, 14(8), 3835–3873. DOI: 10.5194/essd-14-3835-2022
- Engel B. (2022). The Concept of the Socialist City. *International Planning History Society Proceedings*, 663–678 Pages. DOI: 10.7480/IPHS.2022.1.6516
- Germano M., Piomelli U., Moin P. and Cabot W.H. (1991). A dynamic subgrid-scale eddy viscosity model. *Physics of Fluids A: Fluid Dynamics*, 3(7), 1760–1765. DOI: 10.1063/1.857955
- Glazunov A.V. (2018). Numerical simulation of turbulence and transport of fine particulate impurities in street canyons. *Numerical Methods and Programming (Vychislitel'nye Metody i Programirovanie)*, 1(55), 17–37. DOI: 10.26089/NumMet.v19r103
- Grylls T., Le Cornec C.M.A., Salizzoni P., Soulhac L., Stettler M.E.J. and Van Reeuwijk M. (2019). Evaluation of an operational air quality model using large-eddy simulation. *Atmospheric Environment: X*, 3, 100041. DOI: 10.1016/j.aeaoa.2019.100041
- Holmes N.S. and Morawska L. (2006). A review of dispersion modelling and its application to the dispersion of particles: An overview of different dispersion models available. *Atmospheric Environment*, 40(30), 5902–5928. DOI: 10.1016/j.atmosenv.2006.06.003
- Jiang R., Xie C., Man Z., Afshari A. and Che S. (2023). LCZ method is more effective than traditional LUC method in interpreting the relationship between urban landscape and atmospheric particles. *Science of The Total Environment*, 869, 161677. DOI: 10.1016/j.scitotenv.2023.161677
- Kadantsev E., Mortikov E. and Zilitinkevich S. (2021). The resistance law for stably stratified atmospheric planetary boundary layers. *Quarterly Journal of the Royal Meteorological Society*, 147(737), 2233–2243. DOI: 10.1002/qj.4019
- Kadaverugu R., Sharma A., Matli C. and Biniwale R. (2019). High Resolution Urban Air Quality Modeling by Coupling CFD and Mesoscale Models: a Review. *Asia-Pacific Journal of Atmospheric Sciences*, 55(4), 539–556. DOI: 10.1007/s13143-019-00110-3
- Kampa M. and Castanas E. (2008). Human health effects of air pollution. *Environmental Pollution*, 151(2), 362–367. DOI: 10.1016/j.envpol.2007.06.012
- Kasimov N., Chalov S., Chubarova N., Kosheleva N., Popovicheva O., Shartova N., Stepanenko V., Androsova E., Chichayeva M., Erina O., Kirsanov A., Kovach R., Revich B., Shinkareva G., Tereshina M., Varentsov M., Vasil'chuk J., Vlasov D., Denisova I. and Minkina T. (2024). Urban heat and pollution island in the Moscow megacity: Urban environmental compartments and their interactions. *Urban Climate*, 55, 101972. DOI: 10.1016/j.uclim.2024.101972
- Kosheleva N.E., Vlasov D.V., Korlyakov I.D. and Kasimov N.S. (2018). Contamination of urban soils with heavy metals in Moscow as affected by building development. *Science of The Total Environment*, 636, 854–863. DOI: 10.1016/j.scitotenv.2018.04.308
- Kurppa M., Hellsten A., Auvinen M., Raasch S., Vesala T. and Järvi L. (2018). Ventilation and Air Quality in City Blocks Using Large-Eddy Simulation—Urban Planning Perspective. *Atmosphere*, 9(2), 65. DOI: 10.3390/atmos9020065
- Lee H. and Mayer H. (2018). Thermal comfort of pedestrians in an urban street canyon is affected by increasing albedo of building walls. *International Journal of Biometeorology*, 62(7), 1199–1209. DOI: 10.1007/s00484-018-1523-5
- Lin Y., An X., Yuan J., Yuan J. and Chen B. (2024). The impact of the urban landscape on PM_{2.5} from LCZ perspective: A case study of Shenyang. *Urban Climate*, 57, 102107. DOI: 10.1016/j.uclim.2024.102107
- Mortikov E.V., Glazunov A.V. and Lykosov V.N. (2019). Numerical study of plane Couette flow: turbulence statistics and the structure of pressure–strain correlations. *Russian Journal of Numerical Analysis and Mathematical Modelling*, 34(2), 119–132. DOI: 10.1515/rnam-2019-0010
- Nourani S., Villalobos A.M. and Jorquera H. (2024). Indoor and outdoor PM_{2.5} in schools of Santiago, Chile: influence of local climate zone (LCZ) environment. *Air Quality, Atmosphere & Health*. DOI: 10.1007/s11869-024-01687-z
- Oke T.R., Mills G., Christen A. and Voogt J.A. (2017). *Urban Climates*, 1st ed. Cambridge University Press. DOI: 10.1017/9781139016476
- Pope III C.A. and Dockery D.W. (2006). Health Effects of Fine Particulate Air Pollution: Lines that Connect. *Journal of the Air & Waste Management Association*, 56(6), 709–742. DOI: 10.1080/10473289.2006.10464485
- Reynolds A.M. and Cohen J.E. (2002). Stochastic simulation of heavy-particle trajectories in turbulent flows. *Physics of Fluids*, 14(1), 342–351. DOI: 10.1063/1.1426392
- Shi Y., Ren C., Lau K.K.-L. and Ng E. (2019). Investigating the influence of urban land use and landscape pattern on PM_{2.5} spatial variation using mobile monitoring and WUDAPT. *Landscape and Urban Planning*, 189, 15–26. DOI: 10.1016/j.landurbplan.2019.04.004

- Starchenko A.V., Danilkin E.A. and Leschinsky D.V. (2023). Numerical Simulation of the Distribution of Vehicle Emissions in a Street Canyon. *Mathematical Models and Computer Simulations*, 15(3), 427–435. DOI: 10.1134/S207004822303016X
- Stewart I.D. and Oke T.R. (2012). Local Climate Zones for Urban Temperature Studies. DOI: 10.1175/BAMS-D-11-00019.1
- Suiazova V.I., Debolskiy A.V. and Mortikov E.V. (2024). Study of Surface Layer Characteristics in the Presence of Suspended Snow Particles Using Observational Data and Large Eddy Simulation. *Izvestiya, Atmospheric and Oceanic Physics*, 60(2), 158–167. DOI: 10.1134/S000143382470021X
- Sützl B.S., Rooney G.G. and Van Reeuwijk M. (2021). Drag Distribution in Idealized Heterogeneous Urban Environments. *Boundary-Layer Meteorology*, 178(2), 225–248. DOI: 10.1007/s10546-020-00567-0
- Tarasova M.A., Debolskiy A.V., Mortikov E.V., Varentsov M.I., Glazunov A.V. and Stepanenko V.M. (2024). On the Parameterization of the Mean Wind Profile for Urban Canopy Models. *Lobachevskii Journal of Mathematics*, 45(7), 3198–3210. DOI: 10.1134/S1995080224603801
- Thomson D.J. and Wilson J.D. (2012). History of Lagrangian Stochastic Models for Turbulent Dispersion. In: J. Lin, D. Brunner, C. Gerbig, A. Stohl, A. Luhar, and P. Webley eds., *Lagrangian Modeling of the Atmosphere*, 19–36. American Geophysical Union. DOI: 10.1029/2012GM001238
- Tkachenko E.V., Debolskiy A.V., Mortikov E.V. and Glazunov A.V. (2022). Large-Eddy Simulation and Parameterization of Decaying Turbulence in the Evening Transition of the Atmospheric Boundary Layer. *Izvestiya, Atmospheric and Oceanic Physics*, 58(3), 219–236. DOI: 10.1134/S0001433822030112
- Varentsov A.I., Imeev O.A., Glazunov A.V., Mortikov E.V. and Stepanenko V.M. (2023). Numerical Simulation of Particulate Matter Transport in the Atmospheric Urban Boundary Layer Using the Lagrangian Approach: Physical Problems and Parallel Implementation. *Programming and Computer Software*, 49(8), 894–905. DOI: 10.1134/S0361768823080248
- Varentsov A.I., Stepanenko V.M., Mortikov E.V. and Konstantinov P.I. (2020). Numerical simulation of particle transport in the urban boundary layer with implications for SARS-CoV-2 virion distribution. *IOP Conference Series: Earth and Environmental Science*, 611(1), 012017. DOI: 10.1088/1755-1315/611/1/012017
- Varentsov M., Konstantinov P., Repina I., Artamonov A., Pechkin A., Soromotin A., Esau I. and Baklanov A. (2023). Observations of the urban boundary layer in a cold climate city. *Urban Climate*, 47, 101351. DOI: 10.1016/j.uclim.2022.101351
- Varentsov M., Samsonov T. and Demuzere M. (2020). Impact of Urban Canopy Parameters on a Megacity's Modelled Thermal Environment. *Atmosphere*, 11(12), 1349. DOI: 10.3390/atmos11121349
- Venter Z.S., Hassani A., Stange E., Schneider P. and Castell N. (2024). Reassessing the role of urban green space in air pollution control. *Proceedings of the National Academy of Sciences*, 121(6), e2306200121. DOI: 10.1073/pnas.2306200121
- Wu B. and Liu C. (2023). Impacts of Building Environment and Urban Green Space Features on Urban Air Quality: Focusing on Interaction Effects and Nonlinearity. *Buildings*, 13(12), 3111. DOI: 10.3390/buildings13123111
- Zhang Y., Ye X., Wang S., He X., Dong L., Zhang N., Wang H., Wang Z., Ma Y., Wang L., Chi X., Ding A., Yao M., Li Y., Li Q., Zhang L. and Xiao Y. (2021). Large-eddy simulation of traffic-related air pollution at a very high resolution in a mega-city: evaluation against mobile sensors and insights for influencing factors. *Atmospheric Chemistry and Physics*, 21(4), 2917–2929. DOI: 10.5194/acp-21-2917-2021
- Zheng X. and Yang J. (2021). CFD simulations of wind flow and pollutant dispersion in a street canyon with traffic flow: Comparison between RANS and LES. *Sustainable Cities and Society*, 75, 103307. DOI: 10.1016/j.scs.2021.103307
- Zhou S., Wang Y., Jia W., Wang M., Wu Y., Qiao R. and Wu Z. (2023). Automatic responsive-generation of 3D urban morphology coupled with local climate zones using generative adversarial network. *Building and Environment*, 245, 110855. DOI: 10.1016/j.buildenv.2023.110855
- Zwozdziak A., Gini M.I., Samek L., Rogula-Kozłowska W., Sowka I. and Eleftheriadis K. (2017). Implications of the aerosol size distribution modal structure of trace and major elements on human exposure, inhaled dose and relevance to the PM_{2.5} and PM₁₀ metrics in a European pollution hotspot urban area. *Journal of Aerosol Science*, 103, 38–52. DOI: 10.1016/j.jaerosci.2016.10.004